

Supplementary Materials for *Rock glacier composition and structure from radio wave speed analysis with dipping reflector correction*

Tyler M. Meng, Eric I. Petersen, and John W. Holt

The figures and tables below provide additional context and details to support the main body of the manuscript. The full set of data and code used for the analysis presented in the paper can be found after publication on the University of Arizona Data Repository at the following doi: [10.25422/azu.data.19495178](https://doi.org/10.25422/azu.data.19495178).

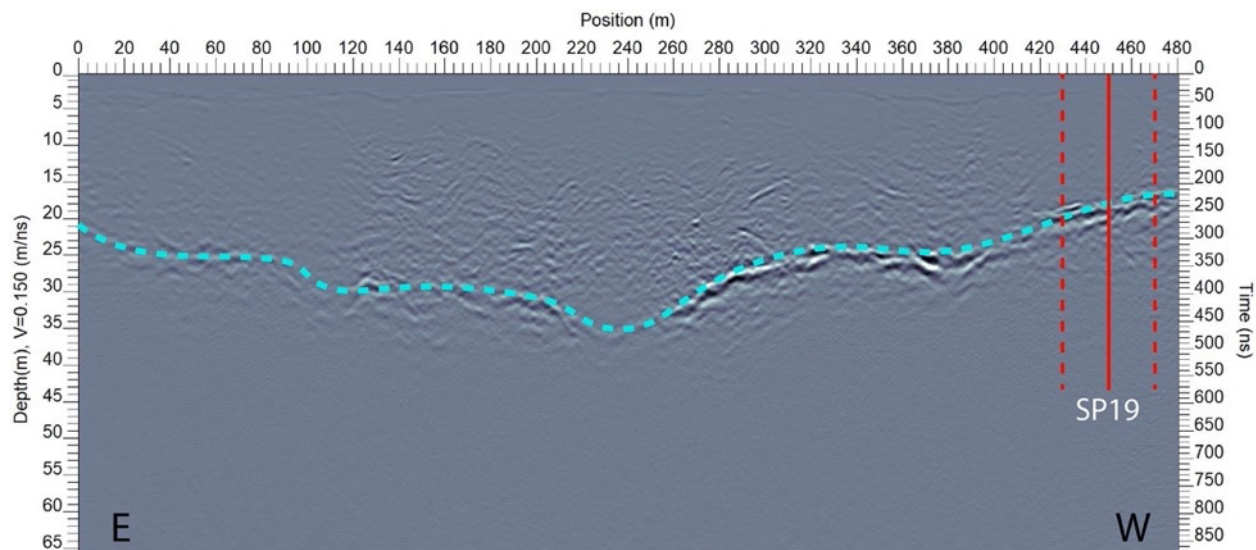


Figure S1: Full 50 MHz common offset transect across the toe of Sourdough Rock Glacier, showing the location of common midpoint SP19 with its sample area (solid and dashed red lines). This gives context for Figure 5b and shows an example of the reflection (dashed blue line) that was interpreted as the rock glacier base and used for the thickness measurements shown in Figure 7.

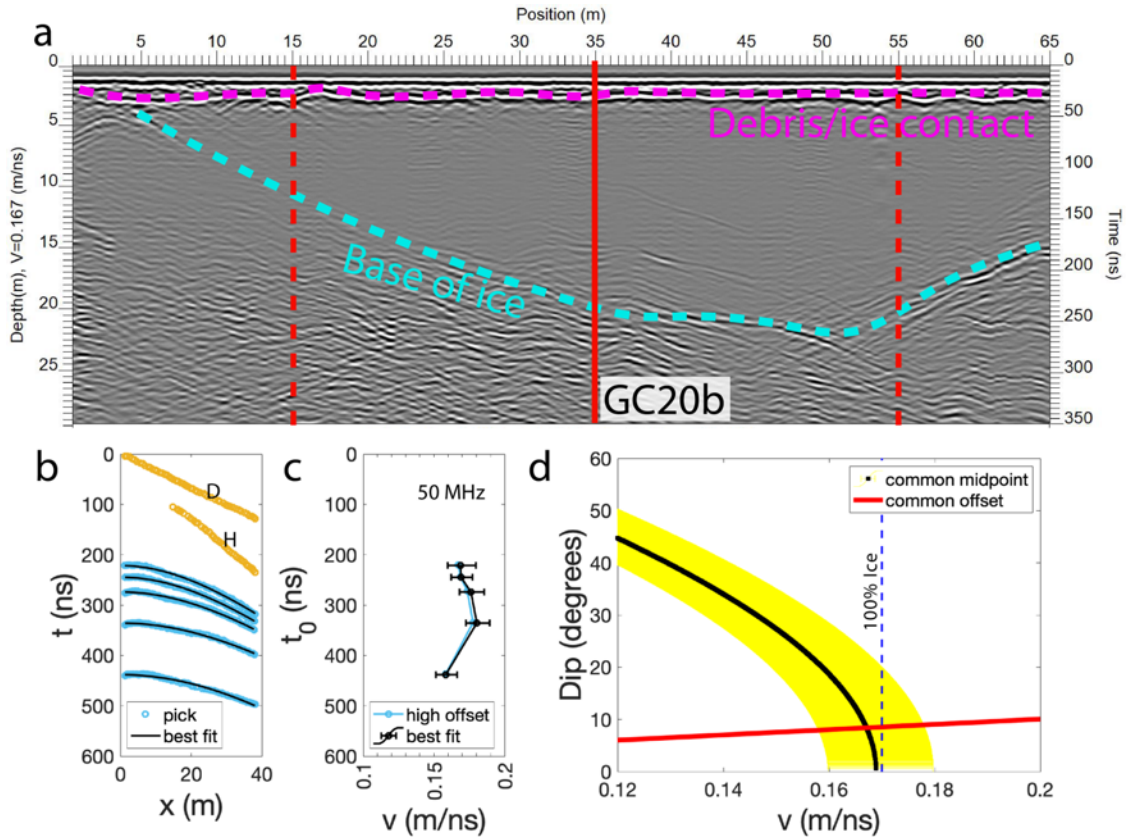


Figure S2: 50 MHz CMP analysis results at Galena Creek location GC20b indicating a wave speed of about 0.168 m ns^{-1} . This is consistent with the results found at GC20a, which is ~ 15 m away but overlies a steeper portion of the reflector.

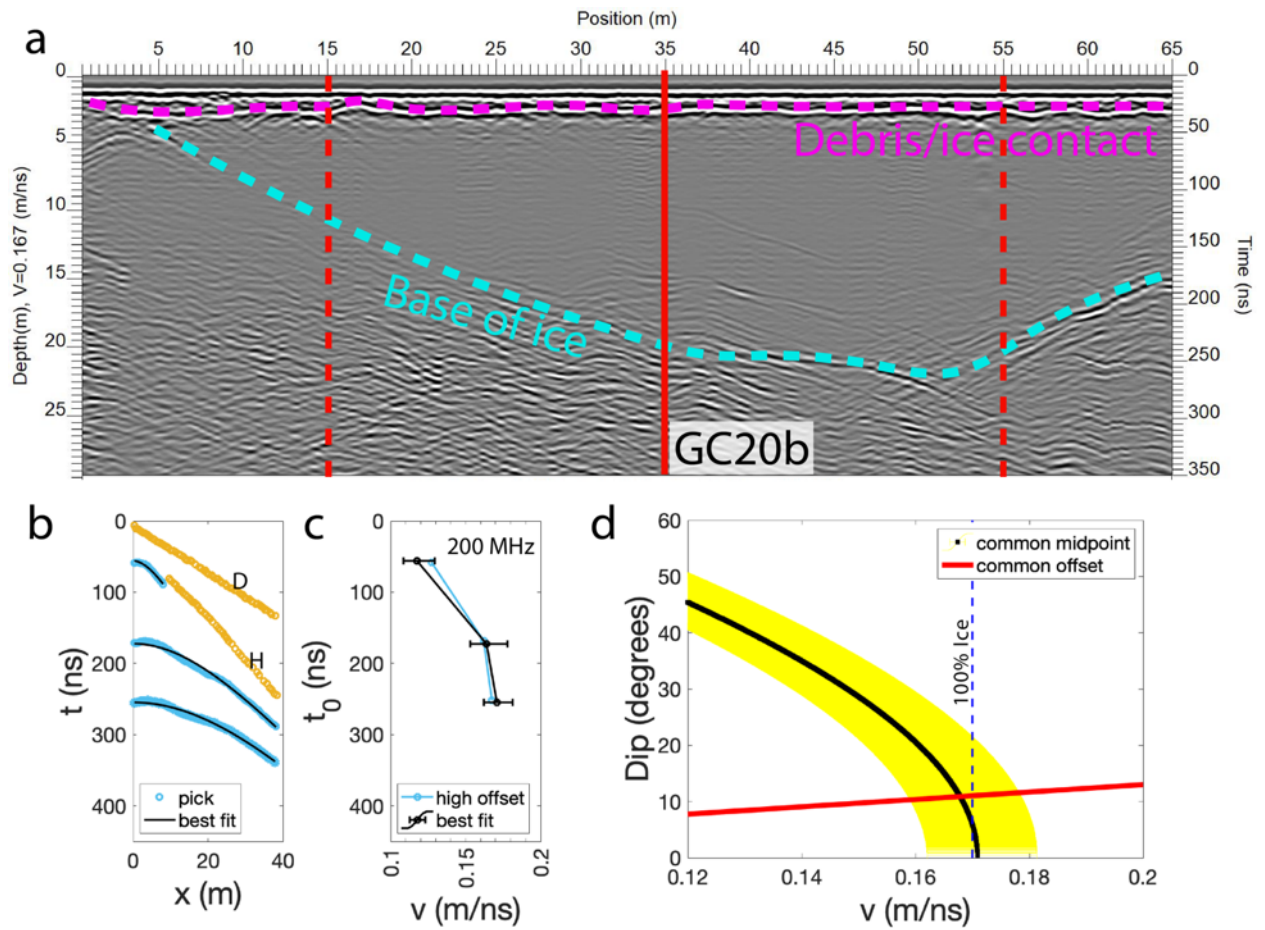


Figure S3: 200 MHz CMP analysis at GC20b indicates a wave speed of about 0.168 m ns^{-1} , further supporting the previous surveys at GC20a and GC20b.

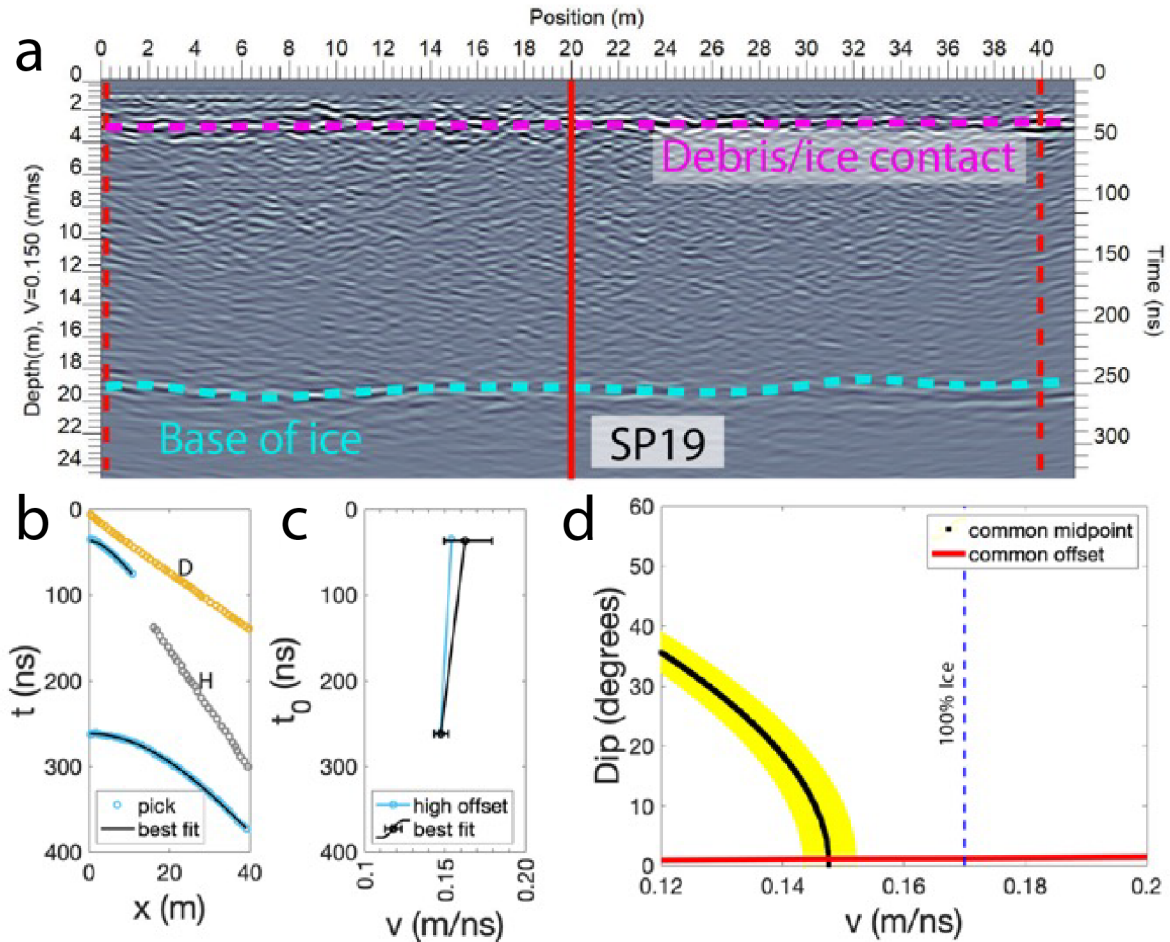


Figure S4: (a) 200 MHz common offset radargram collected in August 2021 at location SP19 (previously surveyed in March 2019) showing interpretations of the base of the debris and the rock glacier along with the orientation of the CMP survey. (b) Picked horizons from the August 2021 CMP. The gold line labeled “D” shows the direct arrival at 200 MHz and the hyperbolic picks show the least squares fits to 200 MHz reflectors. The gray horizon labeled “H” was observed in the 50 MHz CMP at this location and is interpreted to be a headwave caused by refraction along the debris/ice interface, where the wave speed of the underlying medium is approximately 0.145 m ns^{-1} . This refraction may also interfere with interpretation of the shallow debris/ice reflection. (c) Best fit parameters of each reflection according to least squares analysis. (d) Dip angle correction for wave speed; since the basal reflector is very flat here, the bulk wave speed at SP19 is 0.15 m ns^{-1} .

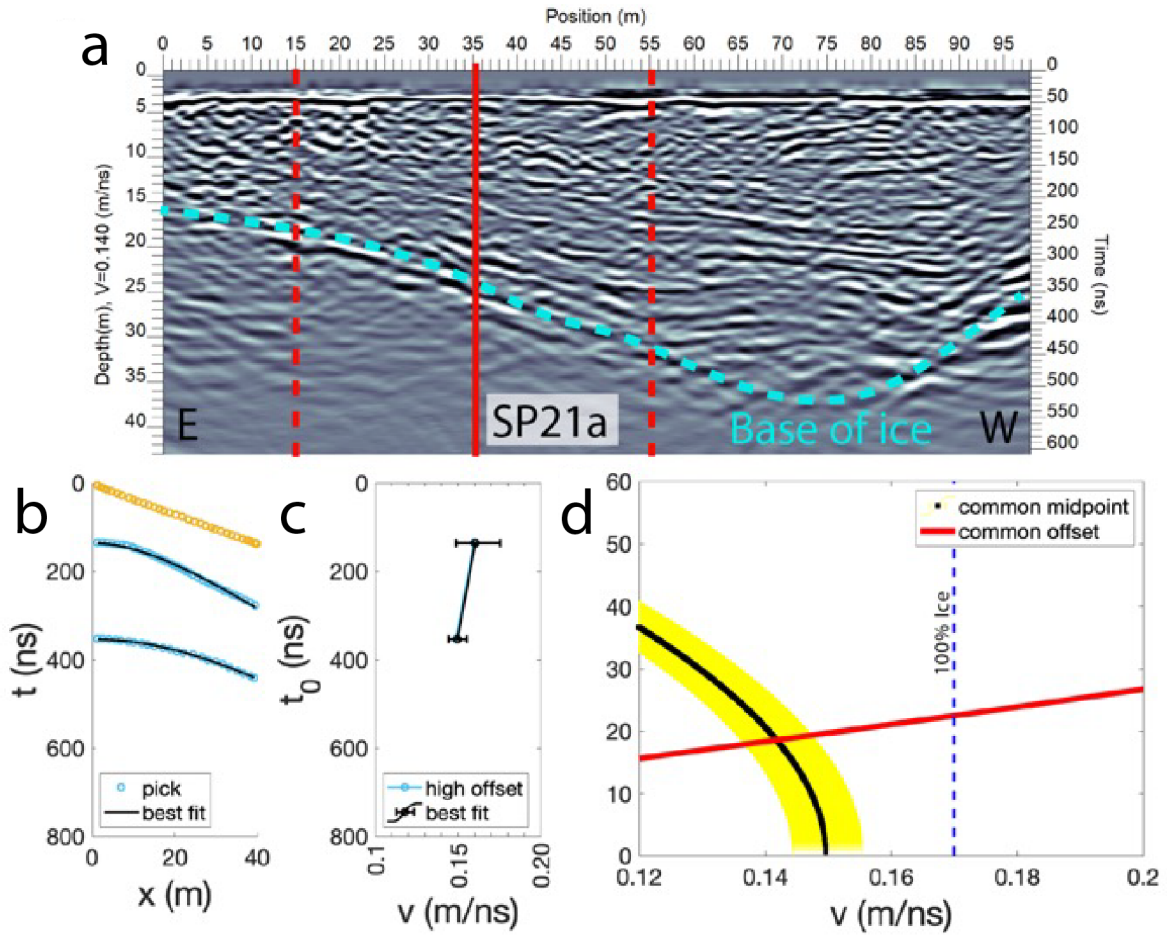


Figure S5: The 50 MHz CMP analysis of August 2021 data in the crossflow direction at Sourdough, Alaska, location SP21a. After correcting for the dipping reflector, the wave speed here is estimated to be 0.14 m ns^{-1} .

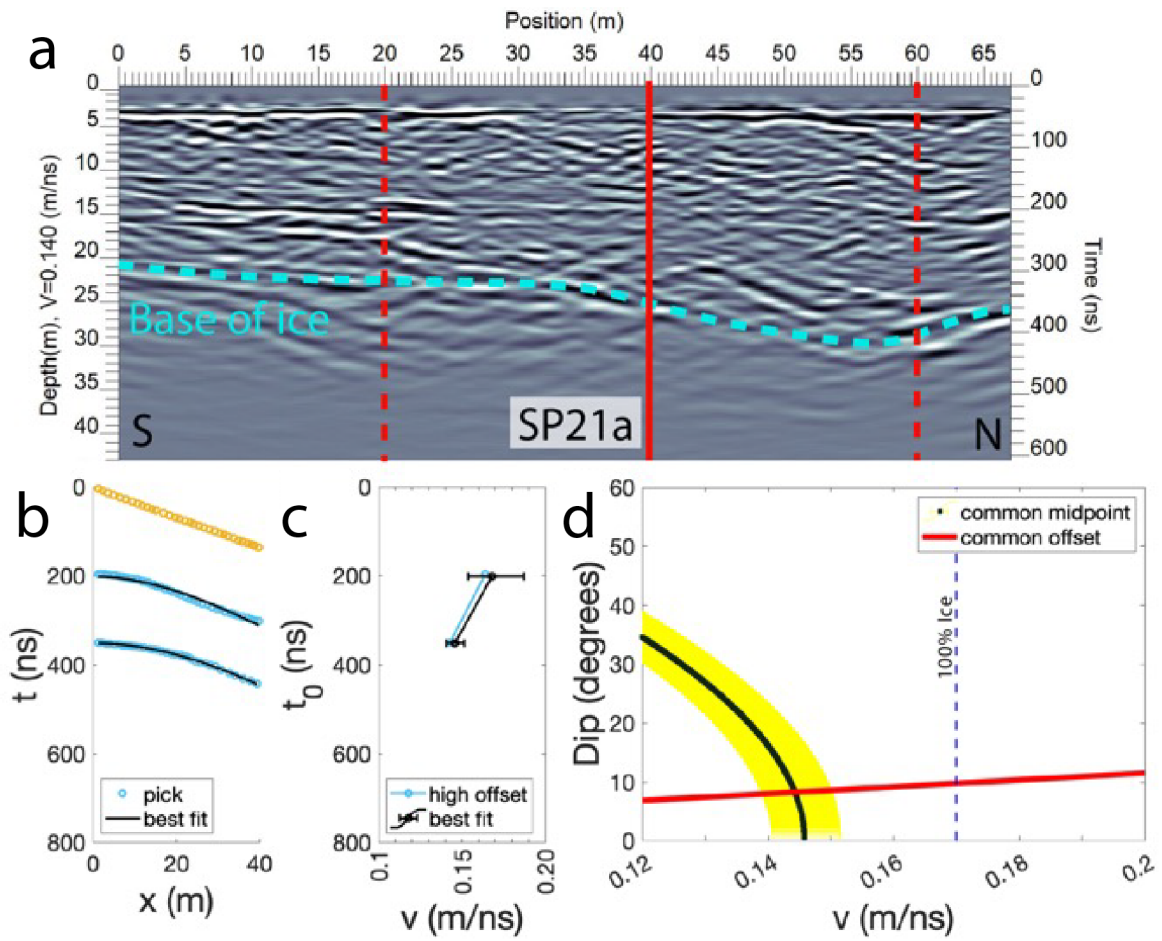


Figure S6: The 50 MHz CMP analysis of August 2021 data in the longitudinal direction at Sourdough, Alaska, location SP21a. After correcting for the dipping reflector, the wave speed here is estimated to be about 0.143 m ns^{-1} .

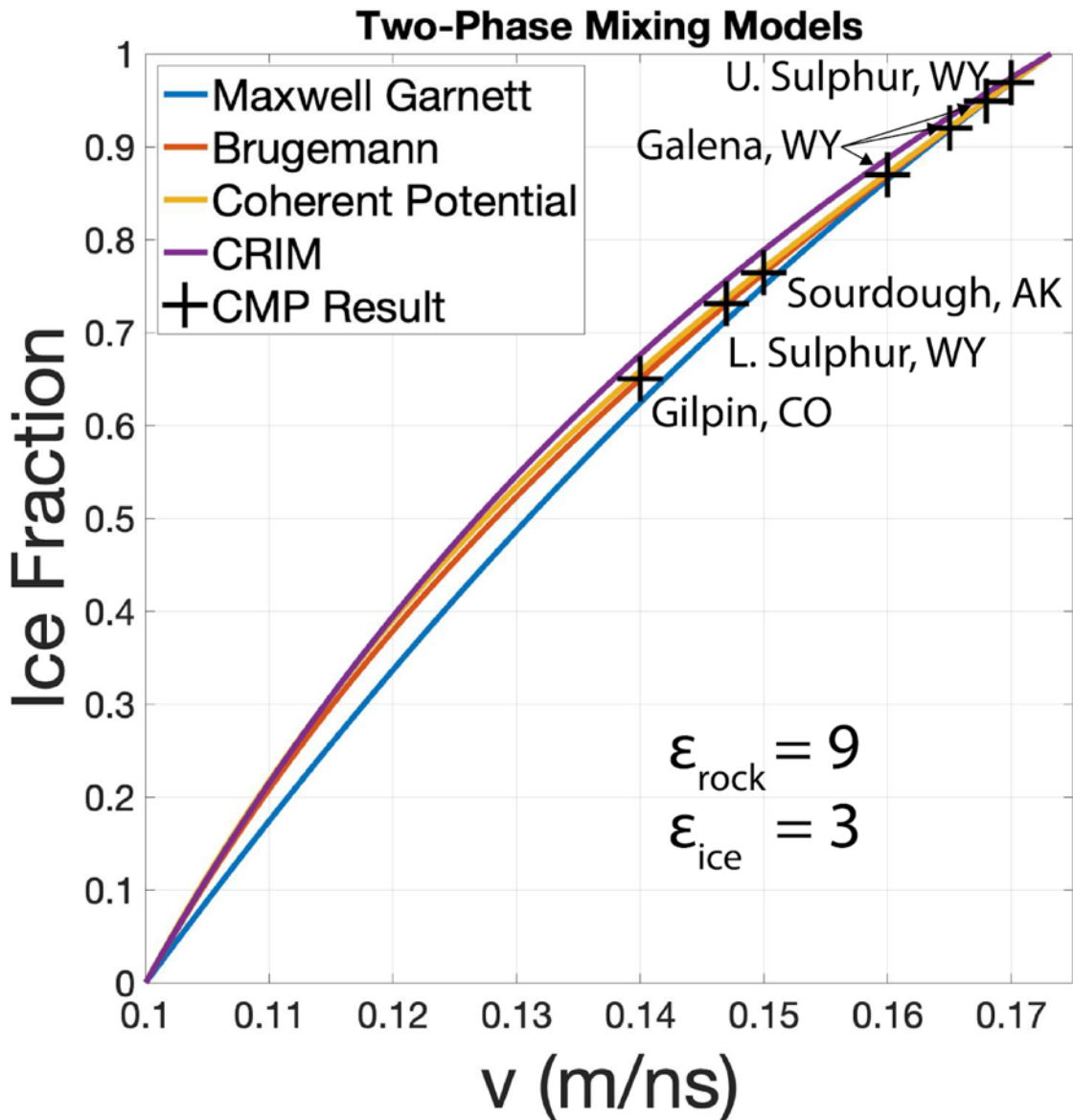


Figure S7: Variations of the unified dielectric mixing models (Sihvola, 2008) and CRIM (Knight and Endres, 1990) plotted with the bulk wave speed results for each location, showing the relationship between wave speed and composition when assuming relative dielectric permittivities of 3 and 9 for ice and rock, respectively. U. Sulphur and L. Sulphur represent upper and lower Sulphur Creek.

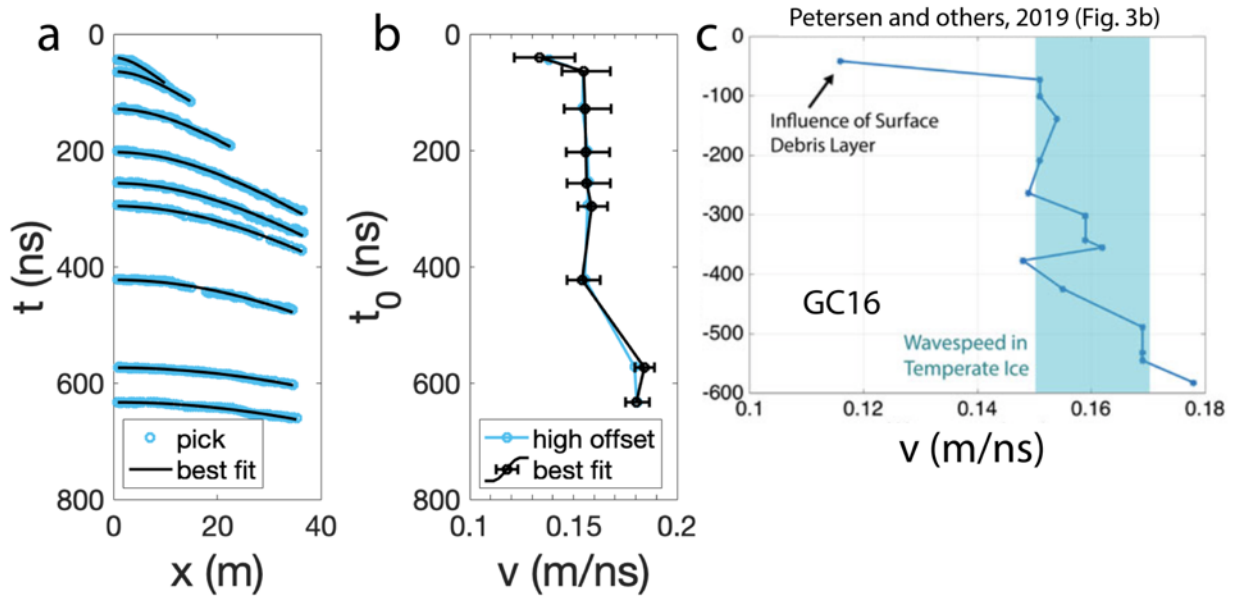


Figure S8: Comparison of wave speed results for the least squares fitting method and the method reported by Petersen and others (2019a), using the data that they collected at location GC16. Both methods produce wave speed profiles that generally increase with depth and average about 0.16 m ns⁻¹, although the noise in the two profiles appears to be represented differently.

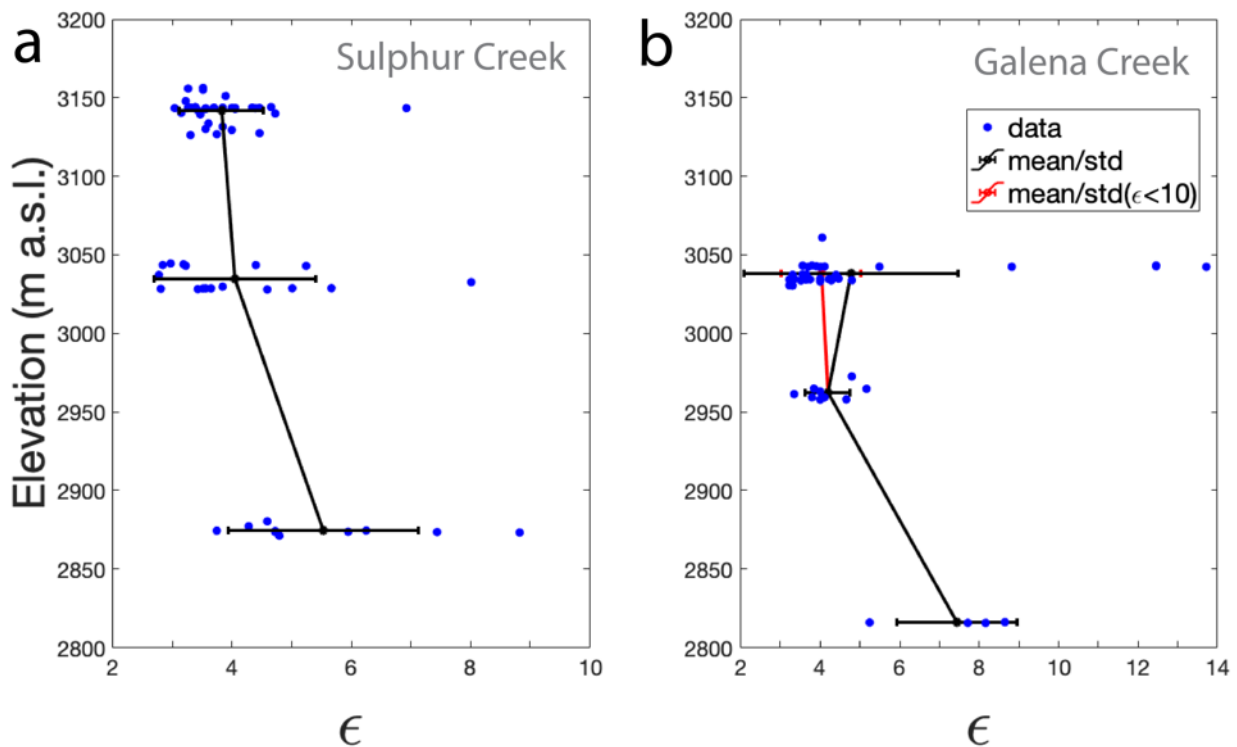


Figure S9: Dielectric constants derived via diffraction hyperbolas vs. surface elevation of measurement location at Sulphur Creek (a) and Galena Creek, WY (b). The trend of increasing dielectric constant with decreasing elevation is consistent with a lower ice fraction moving down-glacier.

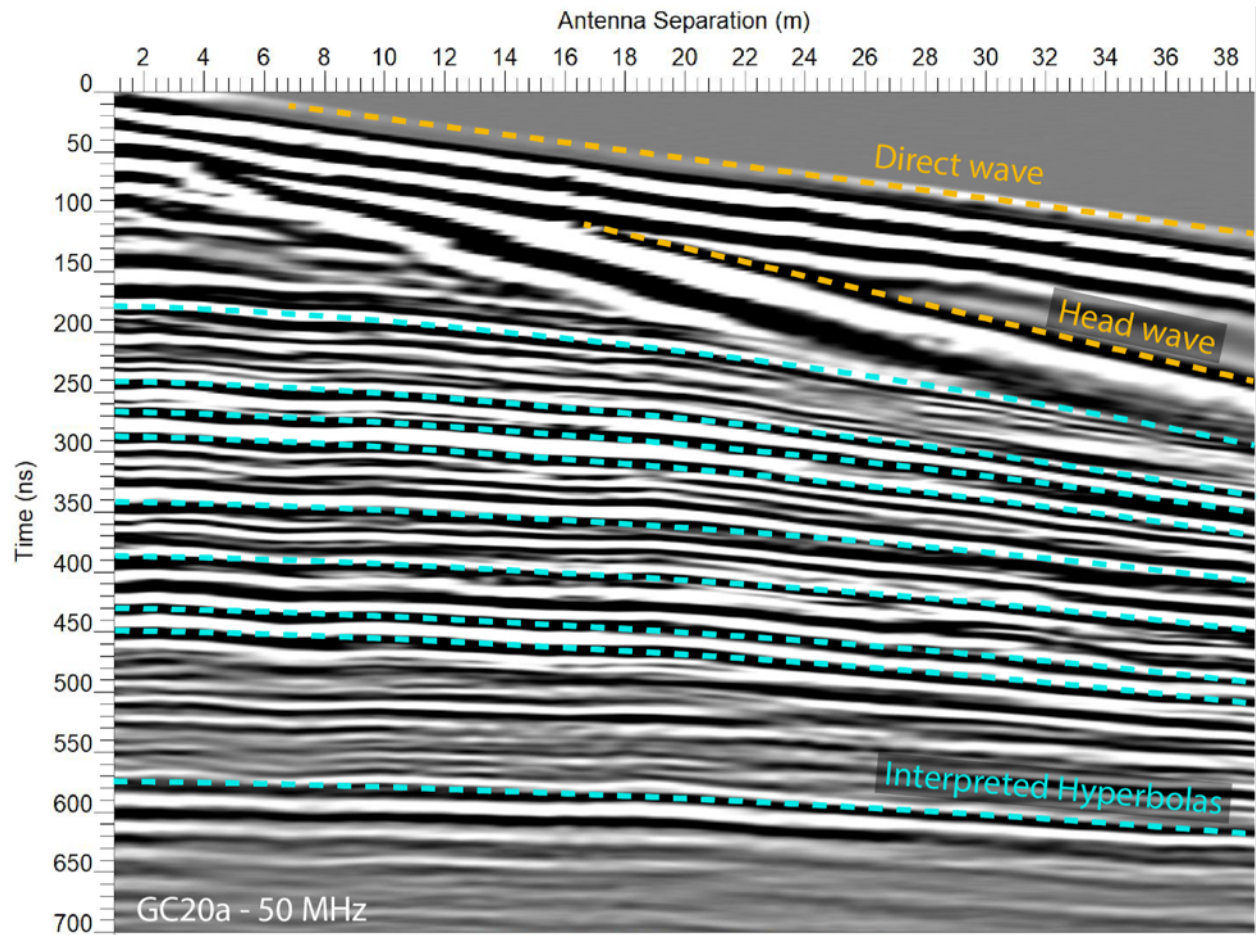


Figure S10: Example of a CMP section (GC20a, corresponding to Figure 8b) displaying a head wave arrival due to refraction at the debris/ice interface and representing another indication of radio wave speed. Interpreted horizons used in the analysis are also labeled in blue.

Table S1 - GPR Acquisition Parameters

a. Common offset antenna configurations

	Summer			Winter
	50 MHz	100 MHz	200 MHz	50, 100, & 200 MHz
Antenna offset	2 m	1 m	0.5 m	1 m
Step size	0.5 m	0.2 m	0.1 m	<i>continuous</i>
Broadside orientation	Perpendicular	Perpendicular	Perpendicular	Parallel

b. Common midpoint antenna configurations

	50 MHz	100 MHz	200 MHz
Start offset	1 m	0.5 m	0.5 m
Step size	0.5 m	0.2 m	0.2 m